Journal of Geodesy manuscript No.
(will be inserted by the editor)

Tuning a gravimetric quasigeoid to GPS-levelling by non-stationary least-squares collocation

N. Darbeheshti · W.E. Featherstone

Received: date / Accepted: date

Abstract This paper addresses implementation issues in order to apply non-stationary least-squares collocation (LSC) to a practical geodetic problem: fitting a gravimetric quasigeoid to discrete geometric quasigeoid heights at a local scale. This yields a surface that is useful for direct GPS heighting. Non-stationary covariance functions and a non-stationary model of the mean were applied to residual gravimetric quasigeoid determination by planar LSC in the Perth region of Western Australia. The non-stationary model of the mean did not change the LSC results significantly. However, elliptical kernels in non-stationary covariance functions were used successfully to create an iterative optimisation loop to decrease the difference between the gravimetric quasigeoid and geometric quasigeoid at 99 GPS-levelling points to a user-prescribed tolerance.

Keywords Least squares collocation (LSC) · non-stationary covariance functions · elliptical kernel convolution · gravimetric quasigeoid · geometric quasigeoid

N. Darbeheshti
Western Australian Centre for Geodesy and The Institute for Geoscience Research, Curtin University of Technology, GPO Box U1987, Perth 6845, Australia
Fax: +61 (0)8 9266 2703; E-mail: neda.darbehesti@postgrad.curtin.edu.au

W.E. Featherstone
Western Australian Centre for Geodesy and The Institute for Geoscience Research, Curtin University of Technology, GPO Box U1987, Perth 6845, Australia
Fax: +61 (0)8 9266 2703; E-mail: W.Featherstone@curtin.edu.au

1 Introduction

Historically, two different approaches have been applied to fit a gravimetric geoid to a geometric geoid or a gravimetric quasigeoid to a geometric quasigeoid. In this study, we shall only refer to the quasigeoid because this is the surface of interest in Australia (cf. Featherstone 2009). In recent years, the differences between the gravimetric quasigeoid and the geometric quasigeoid at discrete GPS-levelling points have been interpolated to create a surface that is applied to the gravimetric quasigeoid grid. This approach gives a practically useful 'product' for the direct determination of heights from GPS on the local vertical datum (cf. Featherstone 1998), but it is always subject to any deficiencies in the GPS-levelling data used in the surface fitting. Also, a plethora of interpolation techniques have been trialled, with least-squares collocation (LSC) now being a popular choice (e.g., Milbert and Dewhurst 1992, Featherstone 2000, Kuroishi et al. 2002, Featherstone and Sproule 2006).

In the older literature, the fitting [albeit indirectly] was performed as a part of the gravimetric quasigeoid determination process. As an early example, Kearsley (1988) selected the cap-radius for the ring-integration approach by optimising the gravimetric quasigeoid to the geometric quasigeoid at GPS-levelling points. However, the cap-radius chosen in this way was then used over the entire computation area. A similar idea is used in this paper, but we use non-stationary covariance functions to optimise a gravimetric to a geometric quasigeoid during the computation stage, where the covariance functions are tuned to deliver a prescribed difference at each GPS-levelling point.

More recently, Prutkin and Klees (2008) formulated the non-uniqueness of local quasi-geoids computed from terrestrial gravity anomalies by using GPS-levelling as a Cauchy problem for the Laplace equation. This is a similar approach, where the GPS-levelling data are used during the quasigeoid computation process.

Darbeheshti and Featherstone (2009) presented the implementation of the Higdon et al. (1999) method (herein HSK) for non-stationary covariance modelling for the interpolation of residual free air gravity anomalies by LSC. In short, HSK use spatially variant ellipse kernels to build non-stationary covariance functions. However, we suggest that Darbeheshti and Featherstone (2009) is consulted for clarification of the concepts used in this paper. However, there are still unanswered questions relating to the best use of this method more generally in LSC-based physical geodesy:

- How can non-stationary covariance functions be applied when LSC is used for the prediction of different gravity field functionals from one another?
- How much does accounting for non-stationarity of the mean (not just the covariance; cf. Darbeheshti and Featherstone 2009) affect the LSC results?
- How should elliptical kernels be defined for the prediction points? For the case of interpolation, where observation and prediction are the same functional, the statistical analysis of observations is sufficient, but for the case of prediction of the quasigeoid from gravity anomalies, for example, how should the elliptical kernels be designed for the prediction points?

This study tries to answer these questions. It uses the same study area as Featherstone (2000), Claessens et al. (2001), Kirby (2003) and Darbeheshti and Featherstone (2009) because the Darling Fault causes strong non-stationarity in the gravity field across Perth region of Western Australia. For instance, the quasigeoid gradient with respect to a geocentric ellipsoid is extremely steep, rising by as much as 40 cm over only 2 km (200 ppm). In AUSGeoid98 (Featherstone et al. 2001), this steep gradient was handled by using LSC in a separate interpolation stage only over this region (Featherstone 2000). Claessens et al. (2001) and Kirby (2003) later found that the need to apply a posteriori fitting to GPS-levelling originated largely from erroneous ship-track data, which has since been confirmed by comparisons with independent data (Featherstone 2009).

This paper looks at the prediction of a gravimetric quasigeoid from gravity anomalies using non-stationary methods (mean and covariance) in planar LSC. The non-stationary methods for the mean and covariances will be applied separately to examine if non-stationarity of the mean is more critical than non-stationarity of covariances in LSC or vice versa. The model for the non-stationary of the mean will first be applied to planar LSC, then HSK's non-stationary method for covariances will be implemented in planar LSC. The elliptical kernels at the observation points (gravity anomalies) are the same as those used by Darbeheshti and Featherstone (2009). When designing elliptical kernels for the prediction points, the residual geometric quasigeoid at 99 discrete GPS-levelling stations will be used.

2 Geometric quasigeoid in the Perth region

There are algebraic transformations where the orthometric height (H) is subtracted from the ellipsoidal height (h) to give the geoid-ellipsoid separation (N), or the normal height (H_N) is subtracted from the ellipsoidal height to give the quasigeoid-ellipsoid separation, also known as the height anomaly, (ζ). Since the normal-orthometric height (H_N) system is used in Australia (Featherstone and Kuhn 2006), the quasigeoid is used for better consistency:

$$\zeta_{\text{geo}} \doteq h - H_N \tag{1}$$

This will be termed the geometric quasigeoid. The approximation in Eq. (1) is because the different heights are measured along different field-lines, but the differences are probably less than a millimetre over this region, where the maximum topographic height is about 350 m.

There are 99 GPS points available to us in the test area (Fig.1), which are referenced to the GRS80 ellipsoid on the ITRF92 (epoch 1994.0) datum. The dual-frequency GPS baselines were adjusted in 1998 by Landgate (the Western Australian geodetic agency) using Geolab software. The mean of the one-sigma error in the ellipsoidal heights σ_h^2 is 2.4 cm. From inspection of benchmark descriptions, the mean of the one-sigma error in the levelled heights is about 3 cm. Using variance propagation at the two-sigma confidence level, gives an estimated accuracy of the GPS-levelling of 7 cm, which will be used in the sequel.

This data set has been used before by Featherstone (2000), Tziavos and Featherstone (2001) and Kirby (2003). However, there are some minor problems with this data set:

- For the original adjustment of the levelling data to realise the Australian Height Datum (AHD), this region was divided into the 'Perth Metropolitan Zone' and a 'buffer' zone, but the maximum difference between adjustments is only 4 mm (National Mapping Council 1979).
- A comparison of around 200 ITRF2005 (epoch 2000.0) and ITRF92 (epoch 1994.0) ellipsoidal heights across Western Australia (Featherstone 2008) shows a mean absolute difference of 3 cm, but it reached 18 cm in one case. However, this is not an

issue if ITRF92 (epoch 1994.0) ellipsoidal heights are used with the local quasigeoid model presented here.

– There is a widely-acknowledged north-south tilt in the AHD (e.g., Featherstone 2004, 2008 and the many references cited therein).

Figure 1 near here

As a first check of these GPS-levelling data, EGM2008 (Pavlis et al. 2008) was used in linear regressions in latitude and longitude (Fig. 2) show north-south and east-west tilts among the GPS-EGM2008-AHD residuals. The north-south tilt with an R^2 value (R is the correlation coefficient) of ~ 0.20 is more significant than the east-west tilt of $R^2 = \sim 0.01$. The north-south tilt is equivalent to ~ 0.71 mm/km when converting degrees to kilometres (one degree is ~ 111 km at the equator), which roughly agrees with the value of ~ 0.81 mm/km determined by Featherstone (2004) for 48 GPS-AHD points across the southwest of Western Australia, but using AUSGeoid98 instead of EGM2008. Featherstone (2008) obtained a lower north-south tilt of ~ 0.27 mm/km with 243 GPS-AHD points across the whole of Western Australia, but used a GRACE-augmented version of AUSGeoid98.

Figure 2 near here

3 Gravimetric quasigeoid modelling with planar LSC

Since the studies cited in the Introduction were conducted, new data sets are available that improve (shown later) residual gravimetric quasigeoid determination in this region:

– Irregularly spaced land gravity data from Geoscience Australia with an average spatial separation of 3 km (Fig.3);
– The 1-arc-minute DNSC2008GRA (Andersen et al. 2009) grid of free-air anomalies offshore (Fig.3);
– EGM2008 geopotential coefficients to degree and order 2160 (Pavlis et al. 2008);
– A 9-arc-second grid of gravimetric terrain corrections (Kirby and Featherstone 2002) as an approximation of the Molodensky G1 term (cf. Sideris 1990).

Figure 3 near here

Figure 4 is a flowchart illustrating the steps in the gravimetric quasigeoid determination with planar LSC. The *surface* command in the GMT (Generic Mapping Tools)

package (Wessel and Smith 1998; http://gmt.soest.hawaii.edu/) was used for gridding. The tension parameter was fixed to [T = Default = 0, as it gives minimum curvature solution] for all of the *surface* commands used in this paper. Three different grid-sizes of $1' \times 1'$, $2' \times 2'$ and $5' \times 5'$ were tested. The $2' \times 2'$ grid-size appeared to be sufficient in terms of accuracy versus time efficiency. The use of gridded data also avoids ill conditioning or singularities in the numerical inversion of the auto-covariance matrices in LSC, which occurs for closely spaced points. The terrain corrections computed by Kirby and Featherstone (2002) were averaged onto the same grid, then added to the Molodensky free-air gravity anomalies to apply an approximation of the Molodensky G_1 terms (cf. Sideris 1990) needed in quasigeoid determination. After that, EGM2008 gravity anomalies to degree and order 2160 were removed using the HARMONIC_SYNTH program (Holmes and Pavlis 2006). These residual anomalies are in an area bounded between $33.6^\circ S$ and $30.4^\circ S$ and $117.5^\circ E$ and $114.4^\circ E$ for gravimetric residual quasigeoid determination in an area bounded between $32.5^\circ S$ and $31.5^\circ S$ and $116.5^\circ E$ and $115.5^\circ E$. Thus, the target area is smaller than the data area so as to reduce the edge effects (cf. Kirby 2003).

Figure 4 near here

Planar LSC was applied to the residual gravity anomalies to estimate the residual gravimetric quasigeoid, via:

$$\varepsilon_{\zeta_{\mathrm{gra}}} = \mathbf{C}_{\varepsilon_\zeta, \varepsilon_{\Delta g}} \mathbf{C}^{-1}_{\varepsilon_{\Delta g}, \varepsilon_{\Delta g}} \varepsilon_{\Delta g} \tag{2}$$

For the auto-covariance and cross-covariance of $\mathbf{C}_{\varepsilon_\zeta, \varepsilon_{\Delta g}}$ and $\mathbf{C}_{\varepsilon_{\Delta g}, \varepsilon_{\Delta g}}$, the planar covariance functions from Forsberg (1987) were used (Appendix), which are related by the law of covariance propagation. Thus, the two are entirely self-consistent. The use of planar LSC is permitted given the limited areal extent of this study area. Note that this part of our study uses standard LSC; the non-stationary methods will be implemented later.

The empirical covariances of the residual gravity anomalies $\varepsilon_{\Delta g}$ are essential to estimate the parameters of C_0, D and d (defined in the Appendix and in Forsberg (1987)) of the analytical auto-covariance function of $C_{\varepsilon_{\Delta g}, \varepsilon_{\Delta g}}$ and cross-covariance function of $C_{\varepsilon_\zeta, \varepsilon_{\Delta g}}$. The program GPFIT in GRAVSOFT (Forsberg and Tscherning 2008) yields the parameters (C_0, D and d) of the statistical model (covariance function)

to be fitted to the empirical covariances to run the planar LSC (see Figure 5 and Table 1).

Figure 5 near here

Table 1 Parameters describing the fitting of the empirical covariance of the residual gravity anomalies $\varepsilon_{\Delta g}$ with the planar covariance model of Forsberg (1987)

No. of data	Mean(mGal)	C_0(mGal^2)	D(km)	d(km)
9118	-0.83	10.51	4	8

There does not appear to be a standardised convention for the size of neighbourhood search in LSC. To be on the safe side, we set the neighbourhood search out to the point where the empirical covariances tended to be zero. The empirical covariances of the residual gravity anomalies in this particular data set tend to zero after $\sim 40'$ ($\sim$74 km)(cf. Figure 5). Hence, our planar LSC uses a neighbourhood search of $40'$ around each point to compute the residual gravimetric quasigeoid $\varepsilon_{\zeta_{\text{gra}}}$ by planar LSC. The results will be presented later (Section 4.2, Table 3), next to the results from the non-stationary LSC.

4 Using non-stationary mean and covariances in planar LSC

4.1 *Testing non-stationarity of the mean*

The standard (planar or spherical) LSC formulation is based on the zero-mean assumption of the vector of observations (e.g., Moritz 1980). Table 2 shows the mean and variance of the observation vector (residual gravity anomalies $\varepsilon_{\Delta g}$) for a representative sample of our 99 GPS-levelling prediction points. It shows how much the mean of each observation vector is offset from zero, and how the observation vector is non-stationary: the larger variance indicates that data is more scattered about the mean, thus, it is a very coarse measure of non-stationarity of the mean.

Non-stationarity models of the spatial mean have been applied in geostatistics for many years (e.g., Wackernagel 2003). One of the practically useful methods is the adaptation of ordinary Kriging (OK) to account for non-stationarity of the mean, which was introduced by Deutsch and Journel (1998) in the *GSLIB* software. OK amounts

Table 2 A typical sample of the mean and variance of the observation vectors for the GPS-levelling prediction points. The mean was computed by taking the mean gravity anomaly for all 1680 residual gravity anomalies in a cap of $40'$ radius about each of the 99 GPS-levelling points. The variance was computed for the same areas using the square of the standard deviation about the mean.

Point No.	Mean(mGal)	C_0(mGal^2)
53	-1.066	15.413
54	-1.916	20.323
58	-1.861	16.261
59	-1.571	15.410
60	-0.435	14.506
61	-0.129	12.576
62	-0.441	15.094
63	-0.878	16.451
76	-0.722	13.590
77	-1.560	18.873
78	-1.010	18.518
79	-0.159	12.444
80	-0.328	14.553
81	-1.518	20.073
82	0.082	11.105
83	-0.522	13.335
84	-1.288	17.916

to re-estimating, at each new location, the mean m as used in the simple Kriging (SK) expression. The only difference between SK and LSC is that SK assumes that the mean is known, while LSC is based on the zero-mean assumption. Some authors (e.g., You 2006) simply reduce the mean as a trend from the data, which basically comes from geostatistics. Cressie (1993) suggested using the median of the data instead, because by removing the mean, there is a danger of adding a bias to the data.

Because OK is most often applied within moving-search neighbourhoods (Deutsch and Journel 1998), i.e., using different subsets for different locations, the implicit re-estimated mean depends on location. Hence, OK as applied within moving data neighbourhoods is already a non-stationary algorithm in the sense that it corresponds to a non-stationary random field model with varying mean, but stationary covariance. This

ability to locally re-scale the random field model to a different mean value m explains the robustness of the OK algorithm (Chilès and Delfiner 1999).

The idea of using just neighbouring data is derived from Kriging algorithms, but is also commonplace in regional quasigeoid determination from LSC or numerical Stokes integration. The first reason for this is to limit the CPU and computer memory requirements. Furthermore, adopting a global search neighbourhood would require knowledge of the covariance for the largest separation distance between data. The covariance is typically poorly known for distances beyond one-half or one-third of the size of a study area. A third reason for a limited search neighbourhood is to allow local re-scaling of covariance parameters for each computation point (Deutsch and Journel 1998).

To introduce non-stationarity of the mean, the LSC Eq. (3), based on the zero mean assumption,

$$\varepsilon_{\zeta_{\mathrm{gra}}} = \mathbf{C}_{\varepsilon_\zeta,\varepsilon_{\Delta g}}\mathbf{C}^{-1}_{\varepsilon_{\Delta g},\varepsilon_{\Delta g}}\boldsymbol{\varepsilon}_{\Delta g}, \tag{3}$$

changes to

$$\varepsilon_{\zeta_{\mathrm{gra}}} = \mathbf{C}_{\varepsilon_\zeta,\varepsilon_{\Delta g}}\mathbf{C}^{-1}_{\varepsilon_{\Delta g},\varepsilon_{\Delta g}}\boldsymbol{\varepsilon}_{\Delta g} + (1 - \sum(\mathbf{C}_{\varepsilon_\zeta,\varepsilon_{\Delta g}}\mathbf{C}^{-1}_{\varepsilon_{\Delta g},\varepsilon_{\Delta g}}))m(\boldsymbol{\varepsilon}_{\Delta g}), \tag{4}$$

(cf. Deutsch and Journel 1998), where $m(\varepsilon_{\Delta g})$ is the mean value of the residual gravity anomalies for each prediction point (the mean of the neighbourhood of $40'$ around each prediction point). If the mean is zero in Eq. (4), this degenerates the standard LSC formulation of Eq. (3).

The difference between the residual gravimetric quasigeoid heights based on the non-stationary mean LSC of Eq. (4) and the standard zero-mean LSC of Eq. (3) were insignificantly small (of the order millimetres), so are not presented here. Because, in this case, the mean values of the observation vectors for each point are small (cf. Table 2), the zero stationary assumption of the mean does not affect the result much. However, this method might be more effective in cases when the zero stationary assumption of the mean is more strongly contradicted; or in other words, when mean values and variances are more inhomogeneous than in this case-study example. The general Kriging method of Reguzzoni et al. (2005), which accounts for a non-zero mean in LSC, also reached the same conclusion.

4.2 *Testing non-stationarity of the covariances*

The same HSK kernel convolution method used for the interpolation of residual free-air gravity anomalies (Darbeheshti and Featherstone 2009) will be applied here for non-stationary covariances for residual gravimetric quasigeoid prediction in planar LSC. This means that the Euclidean distance of

$$r_{ij}^2 = x_{ij}^2 + y_{ij}^2 = \begin{bmatrix} (x_i - x_j) & (y_i - y_j) \end{bmatrix} \begin{bmatrix} 1 & 0 \\ 0 & 1 \end{bmatrix}^{-1} \begin{bmatrix} (x_i - x_j) \\ (y_i - y_j) \end{bmatrix} \tag{5}$$

for two points $P_i = (x_i, y_i)$ and $P_j = (x_j, y_j)$, usually used to build covariance matrices of $\mathbf{C}_{\zeta,\Delta g}$ and $\mathbf{C}_{\Delta g,\Delta g}$, is replaced with

$$Q_{ij}^2 = x_{ij}^2 + y_{ij}^2 = \begin{bmatrix} (x_i - x_j) & (y_i - y_j) \end{bmatrix} \begin{bmatrix} \frac{1}{2} \left(\Sigma_i + \Sigma_j \right) \end{bmatrix}^{-1} \begin{bmatrix} (x_i - x_j) \\ (y_i - y_j) \end{bmatrix} \tag{6}$$

where

$$\Sigma^{\frac{1}{2}} = \tau \begin{pmatrix} a & 0 \\ 0 & b \end{pmatrix} \begin{pmatrix} \cos\alpha & \sin\alpha \\ -\sin\alpha & \cos\alpha \end{pmatrix} \tag{7}$$

in which a and b are the axes of the ellipse and α is the direction angle (measured anticlockwise from the x-axis) of the major axis of the ellipse.

The same covariance functions of Forsberg (1987) are used for non-stationary LSC (cf. Appendix); so the covariances are still consistent and derived from a basis covariance function by covariance propagation (as in ordinary LSC); the only difference is that the HSK method enforces non-stationarity through the distance function of Eq. (6).

Some conditions (from Darbeheshti and Featherstone 2009) should be considered when designing the scaling factor τ at each observation point:

- Larger-value observations are attributed smaller τ and vice versa. This choice agrees with the presence of the inverse of the covariance matrix of observations in Eq. (3), where the scaling factor τ attributes weight to each observation at each point in LSC;

- τ can not be zero; $\tau = 0$ causes a singularity in the inversion of the covariance matrix of observations in LSC;
- τ should vary smoothly across the region; sudden changes in τ will cause discontinuities in the LSC result;

A critical part of the non-stationary method in Darbeheshti and Featherstone (2009) is the detection of non-stationarity and reflection of this by the elliptical parameters. We have to use as much as geostatistical analysis as possible to detect any evidence of anisotropy and non-stationarity in the data, like looking at the data itself for any source of non-stationarity, e.g., geological features, directional covariance functions, covariance maps (i.e., empirical covariances in all directions represented in 2D), and histograms (Deutsch and Journel 1998). However, the processes of detecting of non-stationarity and attributing the elliptical parameters to each point is largely a subjective issue, which also depends on the experience of the analyst.

Now, the main task is to design elliptical kernels or define elliptical parameters $\{\alpha, a, b\}$ and scaling factors τ for all observation and prediction points. Unlike the non-stationary interpolation example in Darbeheshti and Featherstone (2009), where the observation and prediction points were the same, here the elliptical parameters are designed separately for observation (gravity) and prediction (GPS-levelling) points.

Figure 7 near here

Figure 6 near here

Empirical covariance functions in different directions and a covariance map of the residual anomalies were calculated to detect anisotropy directions (Figs. 7 and 6 respectively). Figure 6 shows two main directions of anisotropy in the residual gravity anomalies. One is azimuth 0° (measured clockwise from the y-axis), which is caused by the Darling Fault (located at 116°E); the residual anomalies along the Darling Fault exhibit values of greater than 5 mGal. Other anisotropy is along azimuth 150°, which is caused by negative residual anomalies in Fig. 8. There is no clear geological origin of this feature.

Figure 8 near here

Directional empirical covariance functions (Fig. 7) show the same anisotropy directions, where two pairs of perpendicular azimuths were searched to define the minor and major axis of the ellipses.

- Azimuths 0° and 90° show the correlation lengths of $d_{0^\circ} = 6.66$ km and $d_{90^\circ} = 5.55$ km, which defines the parameters of the ellipses $\{\alpha = 0^\circ, a = \sqrt{6.66}\text{ km}, b = \sqrt{5.55}\text{ km}\}$ for observations points along the Darling Fault, with residual anomalies more than 5 mGal.
- There is no anisotropic evidence for residual anomalies between -5 mGal and 5 mGal (which are marked with yellow in Fig. 7), thus the circles with the parameters $\{\alpha = 0^\circ, a = b = \sqrt{(d_{0^\circ} + d_{60^\circ} + d_{90^\circ} + d_{150^\circ})/4} = 5.13\text{ km}\}$ were attributed to these points.
- Azimuths of 150° and 60° with correlation lengths of $d_{150^\circ} = 4.44$ km and $d_{60^\circ} = 3.88$ km, define the parameters of ellipses $\{\alpha = 150^\circ, a = \sqrt{4.44}\text{ km}, b = \sqrt{3.88}\text{ km}\}$. These ellipses are attributed to the points with residual anomalies less than -5 mGal, which are marked with dark blue in Fig. 7.

Comparing the average size of ellipses (i.e., $a \times b$) in each category

- For residual anomalies greater than 5 mGal, mainly along the Darling Fault: $\{\alpha = 0^\circ, a = \sqrt{6.66}\text{ km}, b = \sqrt{5.55}\text{ km}\}$: $a \times b = 6.0797\text{ km}^2$
- For residual anomalies between -5 mGal and 5 mGal: $\{\alpha = 0^\circ, a = b = \sqrt{(d_{0^\circ} + d_{60^\circ} + d_{90^\circ} + d_{150^\circ})/4} = 5.13\text{ km}\}$:$a \times b = 5.1300\text{ km}^2$
- For residual anomalies less than -5 mGal: $\{\alpha = 150^\circ, a = \sqrt{4.44}\text{ km}, b = \sqrt{3.88}\text{ km}\}$:$a \times b = 4.1506\text{ km}^2$

shows that the size of ellipses already describes the non-stationarity of residual gravity anomalies in this region. The negative residual anomalies ≤ 5 mGal show the shortest correlation length, mainly to the west of the Darling Fault. Therefore there is no need to vary the scaling factor τ across the region. Thus, τ was fixed to 1.

The next stage is to define the elliptical kernels at the prediction (99 GPS-levelling) points. The elliptical kernels at these prediction points are defined in the same way as for the observation points, i.e., with the assistance of directional empirical covariances and covariance maps. In this case, however, the number of GPS-levelling points is insufficient to calculate a covariance map or directional empirical covariances to reliably detect any anisotropy in the residual geometric quasigeoid. The elliptical parameters in this stage are rely more up on trial and error, but they are chosen carefully to be in the range of elliptical parameters at the observation points. They change slightly from point to point, because the result was very sensitive to the elliptical parameters at

the prediction points. As such, we fixed all three parameters $\{\alpha, a, b\}$ to their average values, and slightly changed the scale parameter τ.

Thus, the parameters of $\{\alpha = 0^\circ, a = 1 \text{ km}, b = 1 \text{ km}\}$ were fixed equally for all elliptical kernels at all GPS-levelling points. The scaling factor τ was allowed to vary at each GPS-levelling point, until the difference of $\varepsilon_{\zeta_{\text{geo}}} - \varepsilon_{\zeta_{\text{gra}}}$ (residual geometric quasigeoid minus residual gravimetric quasigeoid) is obtained for a chosen threshold. In other words, the iteration loop (Fig. 4) will stop when the difference between the geometric and gravimetric quasigeoid at each GPS levelling point is less than a chosen threshold or convergence criterion. To start the optimisation loop in Fig. 4, an initial value is needed for τ, so it was constrained to vary between $0 < \tau < 1$.

However, there is one difference between the variation of τ at the prediction points versus the observation points. The τ at the prediction points contributes to the cross-covariance matrix $\mathbf{C}_{\varepsilon_\zeta, \varepsilon_{\Delta g}}$, which is directly used in planar LSC (Eq. 3), not inversely. Therefore, GPS-levelling points with larger residuals are attributed larger τ. Recall that the aim here is to match the gravimetric quasigeoid estimated by planar LSC to the geometric quasigeoid at the prediction points. In this case, the elliptical kernels in $\mathbf{C}_{\varepsilon_\zeta, \varepsilon_{\Delta g}}$ effectively take the role of weights in LSC. The larger ellipses give larger residual gravimetric quasigeoid heights where there is a larger residual geometric quasigeoid value, and vice versa.

Different criteria should be considered to set the threshold used. Basically, the question here is how much we want to match the gravimetric quasigeoid to geometric quasigeoid at each point. One main concern is how confident we are about the accuracy of GPS-levelling points. In our case, we focused on two criteria: the 7 cm two-sigma average accuracy of the 99 GPS-levelling points and the north-south tilt in the AHD (cf. Section 1).

A threshold of 17 cm was tested first (not presented here) which required four iterations; the threshold of 7 cm adopted here took nine iterations. Table 3 and Fig. 9 compare latitudinale and longitudinale tilts for the 99 residuals with different thresholds compared with stationary LSC. As the threshold is decreased, the tilt is increased until we reach the same pattern in Fig. 2.

Figure 9 near here

Figure 10 shows the elliptical kernels at 99 GPS-levelling points for the last iteration loop with the threshold of 7 cm (cf. Table 4). The number of iterations depends on

Table 3 Latitudinale and longitudinale tilts (in mm/km) for 99 gravimetric-geometric quasigeoid residuals with stationary and non-stationary planar LSC

method	longitude tilt	latitude tilt
stationary LSC	-1.60	0.24
non-stationary LSC with threshold 17cm	0.65	0.97
non-stationary LSC with threshold 7cm	-0.18	0.83

the threshold chosen by the user and the initial values for the elliptical kernels at GPS-levelling points. Generally, the number of iterations increases with a decrease of the threshold and an increase in the number of GPS-levelling points used. A tighter threshold can be used, according to the user's desire, to get a reasonable number of iterations or vice versa. Also, the more GPS-levelling points available, the better the initial elliptical parameters can be estimated.

Table 4 shows the statistics of the stationary and non-stationary LSC methods tested here versus the 99 GPS-levelling points in relation to earlier studies. We acknowledge that independent subsets of the GPS levelling data should be used to give a more objective measure (cf. Featherstone 2000; Featherstone and Sproule 2006). However, the technique described here relies on the GPS-levelling prediction points to define the ellipses in the LSC solution, so no such analysis can be conducted.

Figure 10 near here

Table 4 Descriptive statistics of $(\varepsilon_{\zeta_{\text{geo}}} - \varepsilon_{\zeta_{\text{gra}}})$ (in metres) for the 99 GPS-levelling points for various gravimetric quasigeoid models

Model/method	EGM used	Max	Min	Mean	STD
AUSGeoid98 (Featherstone et al. 2001)	EGM96	0.258	-0.301	-0.600	0.128
Kirby (2003)	EGM96	0.294	-0.330	0.156	0.540
EGM2008 alone	EGM2008	0.311	-0.019	0.126	0.051
LSC with stationary planar covariances	EGM2008	0.217	0.052	0.126	0.037
LSC with non-stationary planar covariances	EGM2008	0.056	-0.066	.0002	0.030

Table 4 shows that planar LSC with non-stationary covariances decreases the magnitude of the differences $(\varepsilon_{\zeta_{\text{geo}}} - \varepsilon_{\zeta_{\text{gra}}})$ versus planar LSC with stationary covariances. Importantly, the difference at each point is less than the user-prescribed 7 cm when

using the non-stationary covariances. Table 4 also shows the differences for previous EGM96-based regional gravimetric quasigeoid models. This shows that EGM2008 has made substantial improvements, even over regional quasigeoid models that added data to EGM96. However, further improvements can be made to EGM2008 by the addition of regional data, but the percentage improvements are smaller relative to EGM96.

Using non-stationary covariances has introduced statistical parameters in addition to the stationary covariance parameters of (C_0, D, d) in Table 1; these are parameters of the elliptical kernels (a, b, α, τ) at the observation and prediction points. These extra parameters were used to tune the gravimetric quasigeoid to the geometric quasigeoid. In other words, the prediction points have the role of control points in non-stationary LSC; the statistical parameters of the non-stationary covariance function change at these points such that, the residual falls below the user-prescribed threshold. The advantage of using non-stationary covariances lies in controlling the threshold at each GPS-levelling point individually; while standard stationary LSC is limited to a fixed solution over the whole data set. In other words, non-stationary LSC provides the advantage of tuning the gravimetric quasigeiod to the geometric quasigeoid by choosing smaller thresholds.

Figure 11 near here

For the estimation of gravimetric qusigeoid on a grid, we need elliptical parameters at every prediction point; thus the elliptical parameters at 99 GPS-levelling points were interpolated over a $2' \times 2'$ grid by *grdmath* command in the GMT (Generic Mapping Tools) package (Wessel and Smith 1998; http://gmt.soest.hawaii.edu/). Figure 11 shows the gravimetric quasigeoid by planar non-stationary LSC, which is tuned to the 99 GPS-levelling points to within 7 cm. From Table 4, this outperforms all previous gravimetric quasigeoids in this region, with respect to these 99 GPS-levelling data.

5 Summary and main conclusions

Approximation solutions, like LSC, are highly dependent on pre-statistical analysis of the input data. Better knowledge of statistical parameters gives a more realistic solution from LSC. An example of such a detailed statistical analysis was conducted in this paper, which is similar to the exploratory data analysis that is very common among geostatisticians for geological data sets.

The numerical tests in this paper showed the effect of non-stationary methods on planar LSC for the prediction of one gravity field functionals from another:

– A non-stationary model of the mean did not change the LSC result significantly for the determination of the gravimetric quasigeoid in the Perth region, but this effect may be more significant where the mean is more non-stationary than for this case-study dataset;
– Non-stationary covariance functions were used to create an iterative optimisation loop to decrease the difference of the residual gravimetric quasigeoid and residual geometric quasigeoid at GPS-levelling points to within a prescribed level of tolerance. This tolerance can be changed according to the user's needs.

Appendix: Local planar covariance models of Forsberg (1987)

Forsberg (1987) introduced a complete set of self-consistent formulas for auto- and cross-covariances for quasi/geoid undulations, gravity disturbances, deflections of the vertical, and second-order gradients. All planar covariance functions from Forsberg (1987) were estimated by taking the derivatives of the auto-covariance of the anomalous potential T. The Forsberg (1987) model for covariance between gravity anomalies is:

$$C_{\Delta g,\Delta g}(r) = -\log(z+r) \tag{8}$$

where

$x = x_2 - x_1$

$y = y_2 - y_1$

$z = z_2 + z_1 + D$

$r = (x^2 + y^2 + z^2)^{1/2}$

For two points $P_1 = (x_1, y_1, z_1)$ and $P_2 = (x_2, y_2, z_2)$ with Euclidean coordinates, located on or above the reference plane. The planar depth parameter D corresponds to the depth to the Bjerhammar sphere.

The corresponding cross-covariance function of quasi/geoid undulations and gravity anomalies is:

$$C_{N,\Delta g} = \frac{r - z\log(z+r)}{\gamma} \tag{9}$$

Singularities in the simple logarithmic covariance functions arise from the inadequacy of the planar approximation at low spatial frequencies. Forsberg's (1987) solution is that any type of covariance function in the final model may expressed as

$$C'(x, y, z_1 + z_2) = f \sum_{i=0}^{3} \alpha_i C(x, y, z_i) \tag{10}$$

where $z_i = z_1 + z_2 + D_i$, with $\alpha_0 = 1$, $\alpha_1 = -3$, $\alpha_2 = 3$, $\alpha_3 = 11$ and C given by the simple logarithmic covariance expressions evaluated using a depth parameter (characteristic distance) $D_i = D + id$. The scaling factor f is:

$$f = C_0 / \log(\frac{D_1^3 D_3}{D_0 D_2^3}) \tag{11}$$

where C_0 and d are the variance and correlation length respectively.

Acknowledgements We thank CC Tscherning and R Forsberg for their great help on the GRAVSOFT software. We are grateful to the organisations that provided the observational data for this research: Geoscience Australia for freely supplying the Australian gravity data via 'GADDS', L Morgan from Landgate, Western Australia for providing the GPS-levelling data, the (EGM) 2008 development team for providing the geopotential coefficients and the HARMONIC_SYNTH software, and the Danish National Space Centre (DNSC) for providing the DNSC2008GRA satellite altimetry data. N Darbeheshti thanks Curtin University of Technology for a CIRTS scholarship and the Department of Spatial Sciences for a living allowance scholarship. WE Featherstone thanks the Australian Research Council for Discovery Project grant DP0663020. We thank the editor and four anonymous reviewers for their constructive comments that allowed us to clarify several points in an earlier version of this manuscript. This is TIGeR publication number xxx (to be inserted after acceptance).

References

Andersen OB, Knudsen P, Berry PAM (2009) The DNSC08GRA global marine gravity field from double retracked satellite altimetry, Journal of Geodesy (online first), DOI: 10.1007/s00190-009-0355-9

Chilès JP, Delfiner P (1999) Geostatistics, Wiley, New York

Claessens SJ, Featherstone WE, Barthelmes F (2001) Experiences with point-mass modelling in the Perth region, Western Australia, Geomatics Research Australia 75:53-86

Cressie N (1993) Statistics for spatial data, Wiley, New York

Darbeheshti N, Featherstone WE (2009) Non-stationary covariance function modelling in 2D least-squares collocation, Journal of Geodesy 83(6):495-508, doi: 10.1007/s00190-008-0267-0

Deutsch CV, Journel AG (1998) GSLIB, Oxford University Press, Oxford

Featherstone WE (1998) Do we need a gravimetric geoid or a model of the base of the Australian Height Datum to transform GPS heights?, The Australian Surveyor 43(4):273-280

Featherstone WE (2000) Refinement of gravimetric geoid using GPS and levelling data, Journal of Surveying Engineering 126(2):27-56, doi: 10.1061/(ASCE)0733-9453

Featherstone WE (2004) Evidence of a north-south trend between AUSGeoid98 and the AHD in southwest Australia, Survey Review 37(291):334-343

Featherstone WE (2008) GNSS-heighting in Australia: current, emerging and future issues, Journal of Spatial Science 53(2):115-133

Featherstone WE (2009) Only use ship-track gravity data with caution: a case-study around Australia, Australian Journal of Earth Sciences 56(2):191-195, doi: 10.1080/08120090802547025

Featherstone WE, Kirby JF, Kearsley AHW , Gilliland JR, Johnston GM, Steed J, Forsberg R, Sideris MG (2001) The AUSGeoid98 geoid model of Australia: data treatment, computations and comparisons with GPS-levelling data, Journal of Geodesy 75(5-6):313-330, doi: 10.1007/s001900100177

Featherstone WE, Kuhn M (2006) Height systems and vertical datums: a review in the Australian context, Journal of Spatial Science 51(1):21-42

Featherstone WE, Sproule DM (2006) Fitting AusGeoid98 to the Australian height datum using GPS-levelling and least squares collocation: application of a cross-validation technique, Survey Review 38(301):573-582

Forsberg R (1987) A new covariance model for inertial gravimetry and gradiometry, Journal of Geophysical Research 92(B2):1305-1310

Forsberg R, Tscherning CC (2008) An overview manual for the GRAVSOFT, University of Copenhagen, Denmark

Higdon D, Swall J, Kern J (1999) Non-stationary spatial modelling. In: Bernardo JM, Berger JO, Dawid AP, Smith AFM (eds) Bayesian Statistics 6. Oxford University Press, Oxford, pp.761-768

Holmes SA, Pavlis NK (2006) Program HARMONIC_SYNTH, a FORTRAN program for very-high-degree harmonic synthesis, National Geospatial-Intelligence Agency, USA

Kearsley AHW (1988) Tests on the recovery of precise geoid height differences from gravimetry, Journal of Geophysical Research 93(B6):6559-6570

Kirby JF (2003) On the combination of gravity anomalies and gravity disturbances for geoid determination in Western Australia, Journal of Geodesy 77(7-8):433-439, doi: 10.1007/s00190-003-0334-5

Kirby JF, Featherstone WE (2002) High-resolution grids of gravimetric terrain correction and complete Bouguer corrections over Australia, Exploration Geophysics 33(3-4):161-165

Kuroishi Y, Ando H, Fukuda Y (2002) A new hybrid geoid model for Japan GSIGEO 2000, Journal of Geodesy 76(8):428-436, doi: 10.1007/s00190-002-0266-5

Milbert DG, Dewhurst WT (1992) The Yellowstone-Hebgen lake geoid obtained through the integrated geodesy approach, Journal of Geophysical Research 97(B1):545-557

Moritz H (1980) Advanced Physical Geodesy, Abacus, Tunbridge Wells

Pavlis NK, Holmes SA, Kenyon SC, Factor JK (2008) An Earth Gravitational Model to Degree 2160: EGM2008, EGU-2008, Vienna, April

Prutkin I, Klees R (2008) On the non-uniqueness of local quasi-geoids computed from terrestrial gravity anomalies, Journal of Geodesy 82(3):147-156, doi: 10.1007/s00190-007-0161-1

Reguzzoni M, Sansò F, Venuti G (2005) The theory of general Kriging, with application to the determination of a local geoid, Geophysical Journal International 162(4):303-314, doi: 10.1111/j.1365-246X.2005.02662.x

Sideris MG (1990) Rigorous gravimetric terrain modeling using Molodensky's operator, manuscripta geodaetica 15(2):97-106.

The Australian Height Datum (AHD) (1979), Rep 8, National Mapping Council of Australia, Canberra

Tziavos IN, Featherstone WE (2001) First results of using digital density data in gravimetric geoid computation in Australia, in: Gravity, Geoid and Geodynamics 2000, MG Sideris (ed.), IAG Symposia Series 123:335-340, Springer, Berlin

Wessel P, Smith WHF (1998) New, improved version of Generic Mapping Tools released, EOS Trans AGU 79(47):579, http://gmt.soest.hawaii.edu/

Wackernagel H (2003) Multivariate Geostatistics: An Introduction with Applications, Springer, Berlin, Germany

You RJ (2006) Local geoid improvement using GPS and levelling data: case study, Journal of Surveying Engineering 132(3):101-107

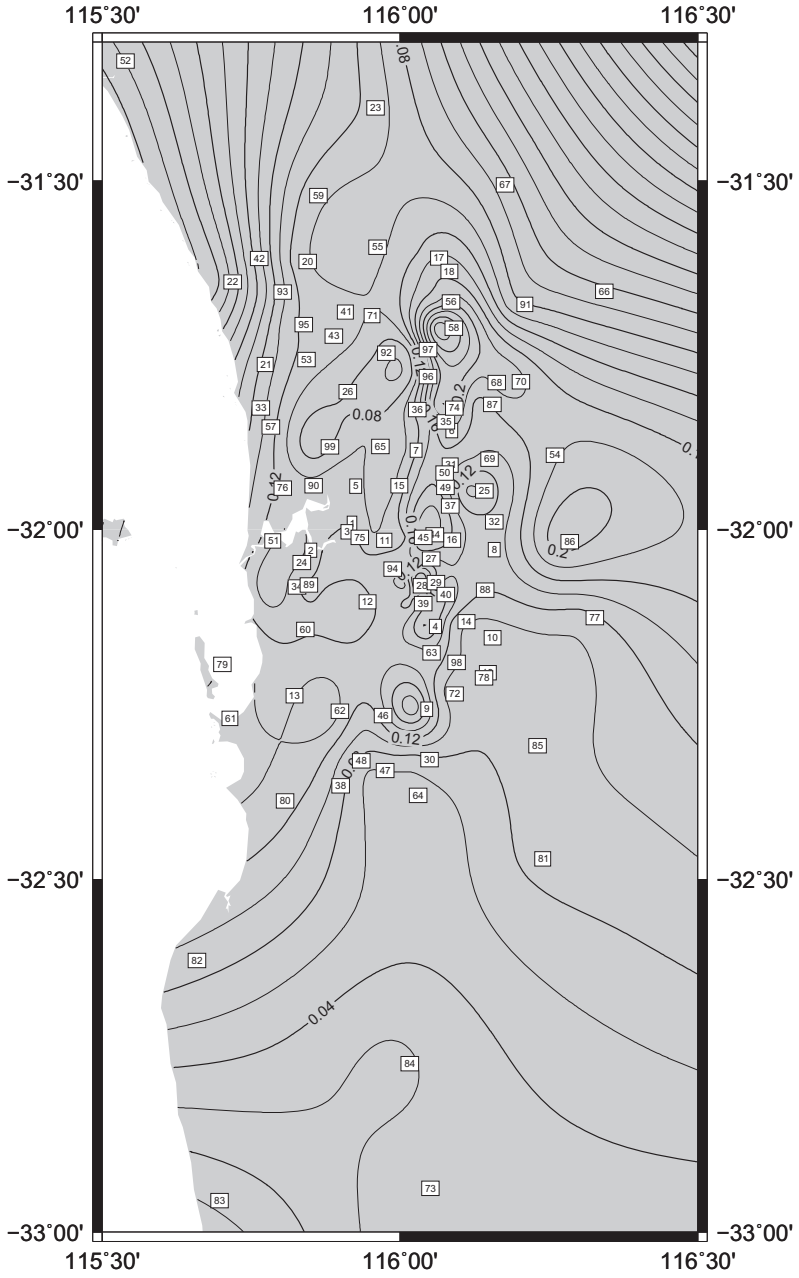

Fig. 1 Distribution of the 99 GPS-AHD points around Perth (white boxes show station number), with the contours of the GPS-AHD quasigeoid residuals ($\varepsilon_{\zeta_{\mathrm{geo}}}$) referenced to EGM2008 to degree 2160 [contour interval 0.02 m, Mercator projection].

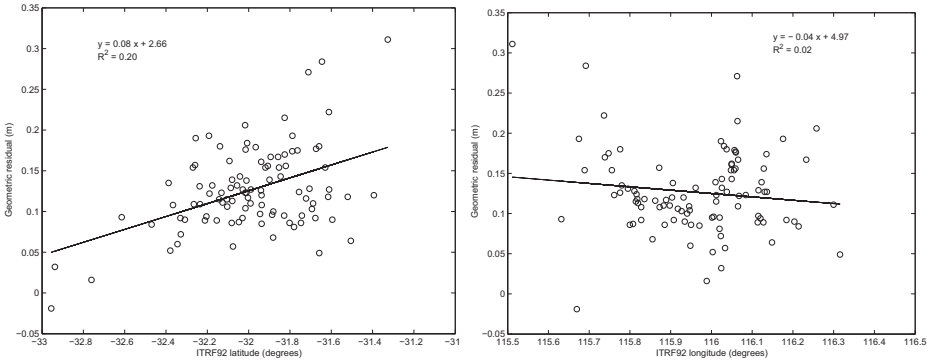

Fig. 2 Linear regression of the 99 GPS-EGM2008-AHD residuals ($\varepsilon_{\zeta_{\text{geo}}}$) in metres versus (left) latitude and (right) longitude in degrees. From the gradient in degrees, this gives tilts of ~ 0.71 mm/km in latitude and ~ -0.38 mm/km in longitude.

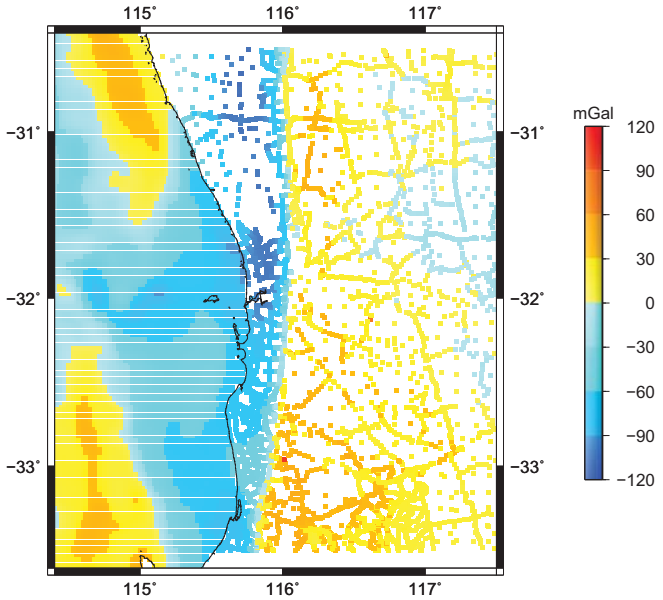

Fig. 3 Coverage of gravity anomalies, which is a combination of irregular land data from Geoscience Australia and 1-arc-minute DNSC2008GRA data offshore [units in mGal; Mercator projection]

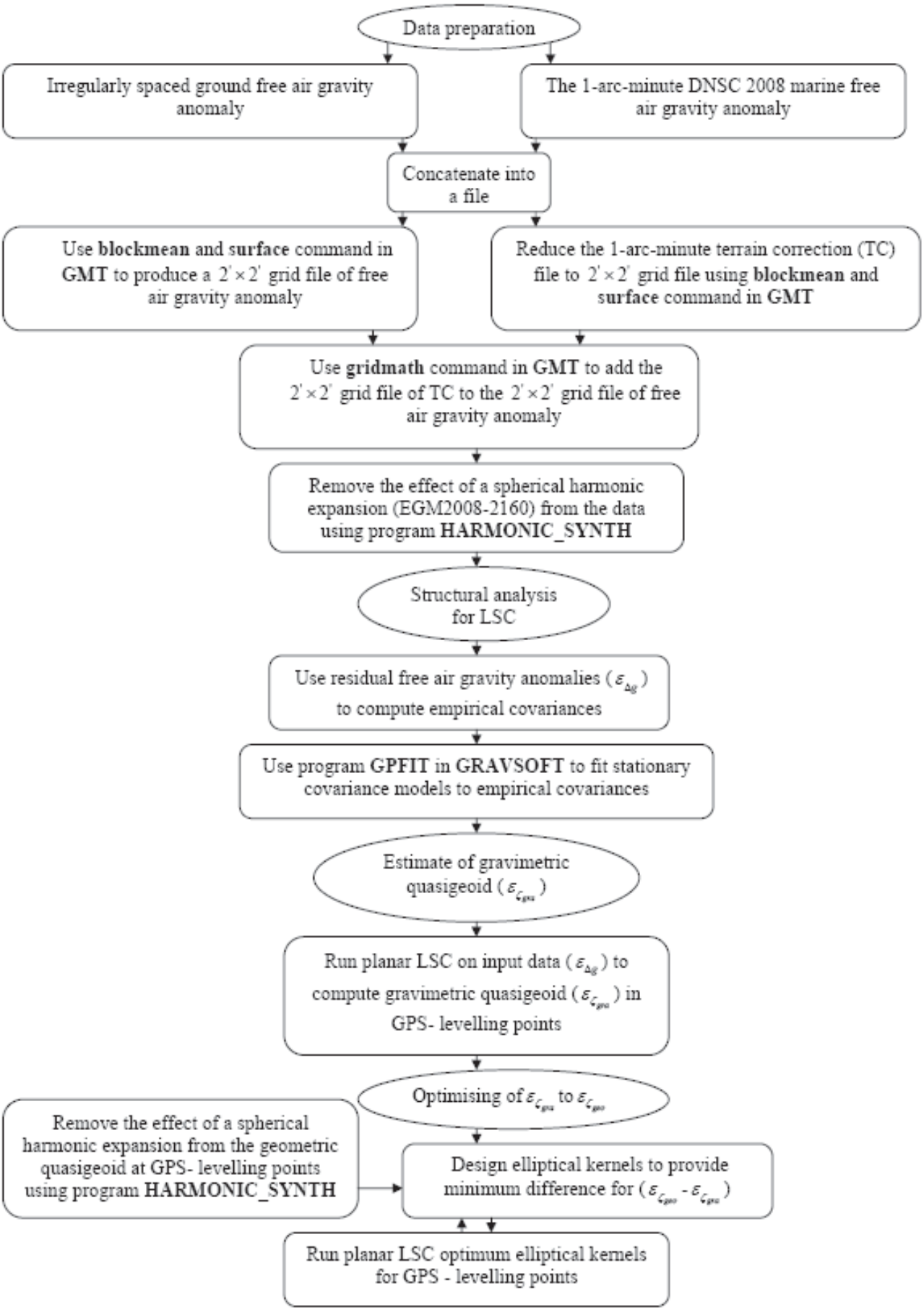

Fig. 4 Flowchart of the planar LSC algorithm for tuning the gravimetric quasigeoid to the geometric quasigeoid. The two last blocks, connected by two opposite arrows, illustrate the optimisation loop used.

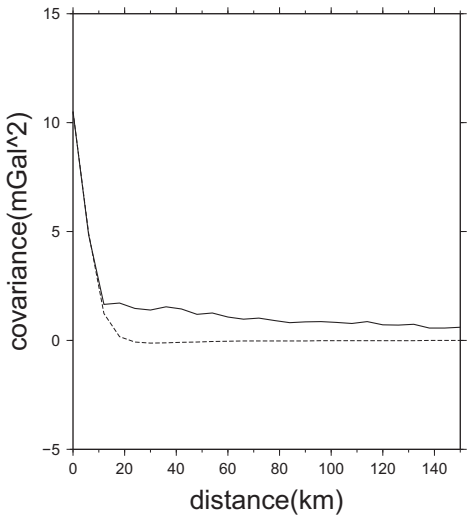

Fig. 5 Fitting of the empirical covariance of residual gravity anomalies $\varepsilon_{\Delta g}$ (solid line) with the planar covariance model of Forsberg (1987) (dashed line)

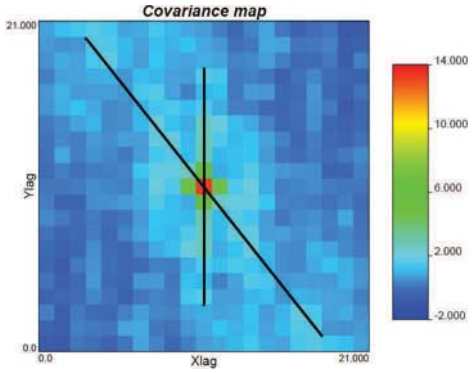

Fig. 6 Covariance map of the residual gravity anomalies $\varepsilon_{\Delta g}$ referenced to EGM2008 [units in mGal^2; linear projection]. The black lines illustrate the directions of anisotropy along the clockwise azimuths 0° and 150°.

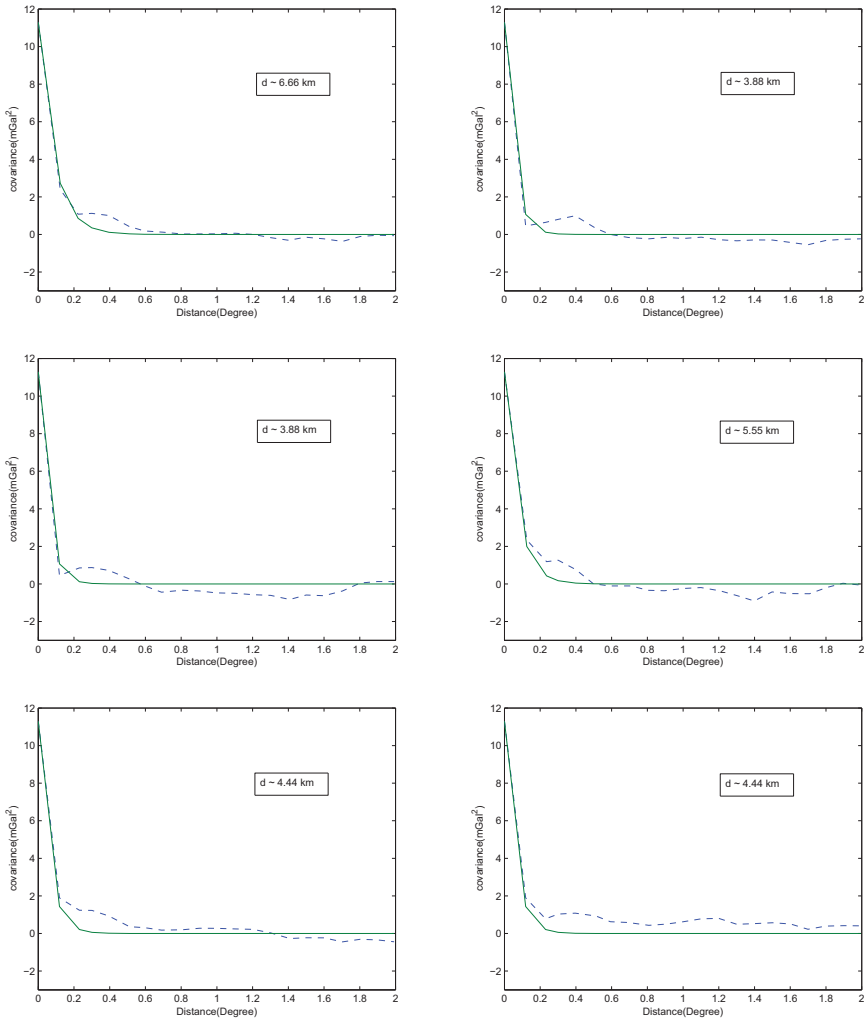

Fig. 7 Empirical covariances (dashed lines in mGal^2) for the residual gravity anomalies $\varepsilon_{\Delta g}$ referenced to EGM2008 for azimuths: 0° (upper left), 30° (upper right), 60° (middle left), 90° (middle right), 120° (lower left) and 150° (lower right). Solid lines illustrate the covariance models fitted to these empirical covariances.

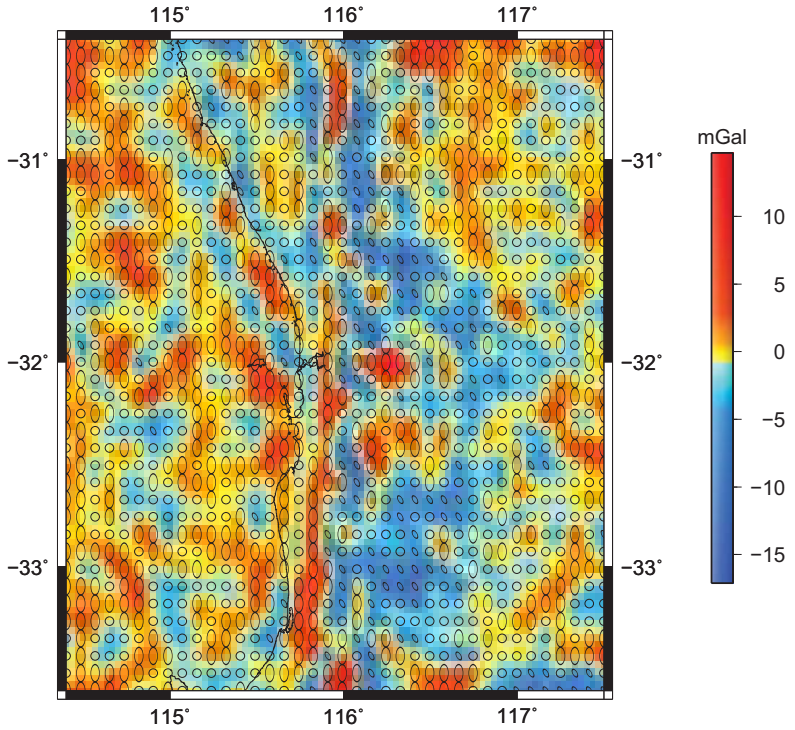

Fig. 8 Elliptical kernels attributed to each observation (gravity) point used to construct the non-stationary auto-covariance matrix $\mathbf{C}_{\varepsilon_{\Delta g},\varepsilon_{\Delta g}}$. The underlying image shows the residual anomalies referenced to EGM2008 [units in mGal; Mercator projection]

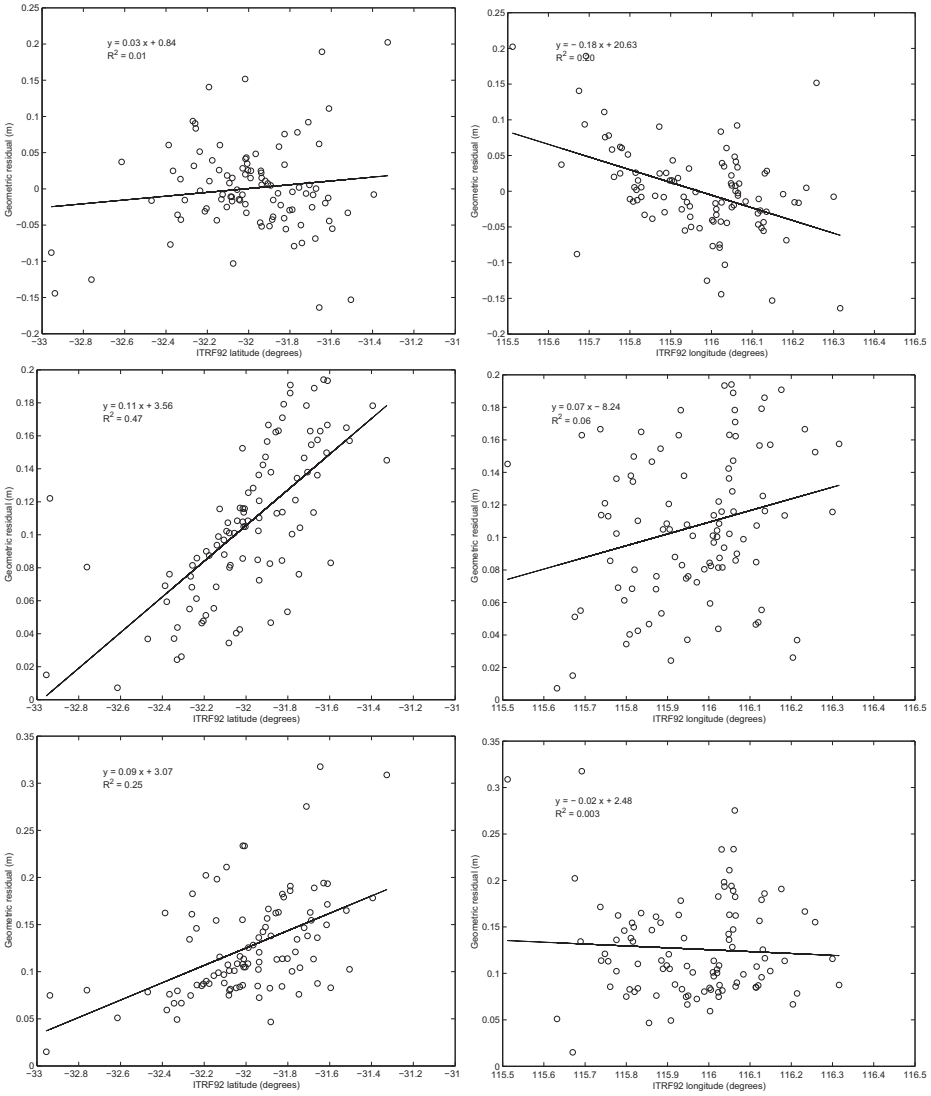

Fig. 9 Linear regression of the 99 gravimetric quasigeoid residuals ($\varepsilon_{\zeta_{\mathrm{gra}}}$) [in metres] versus (left) latitude and (right) longitude [in degrees] for stationary LSC (upper), non-stationary LSC with a threshold of 17 cm (middle) and non-stationary LSC with a threshold of 7 cm (lower).

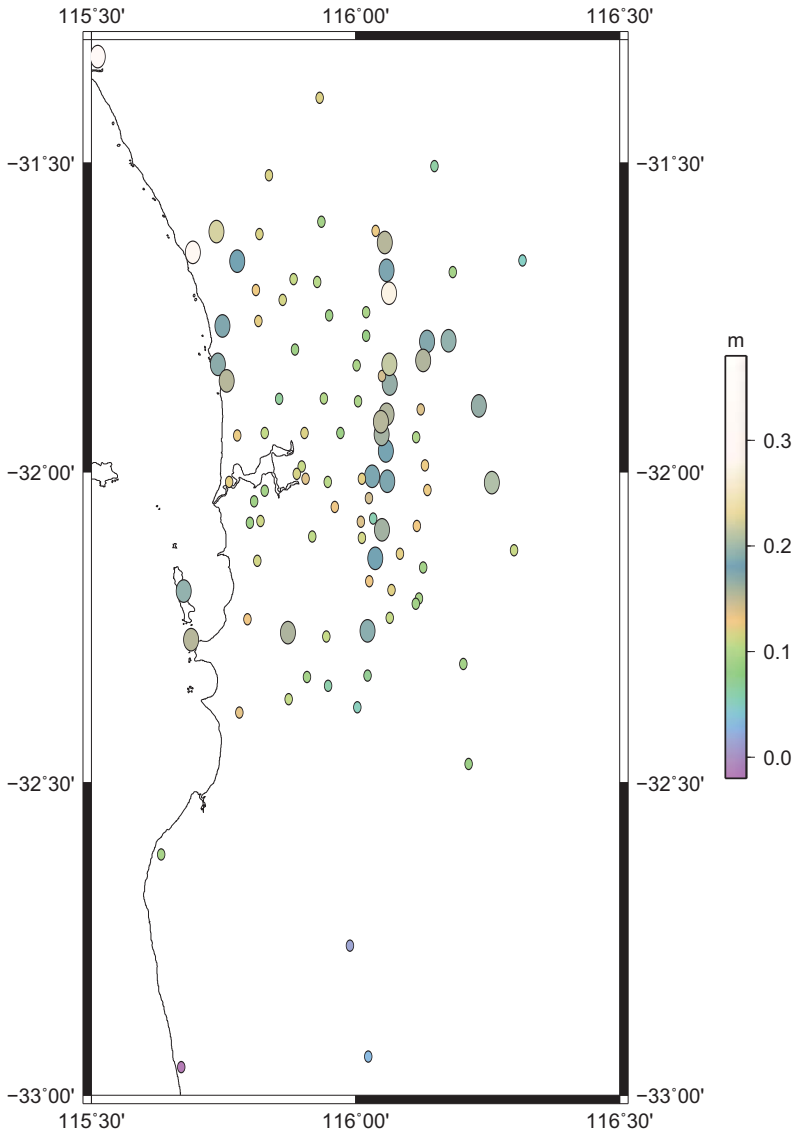

Fig. 10 Elliptical kernels attributed to each prediction (GPS-levelling) point used to construct the non-stationary cross-covariance matrix $\mathbf{C}_{\varepsilon_\zeta,\varepsilon_{\Delta g}}$. The colour inside the ellipses shows the residual geometric quasigeoid heights $\varepsilon_{\zeta_{\text{geo}}}$ referenced to EGM2008 [units in m; Mercator projection]

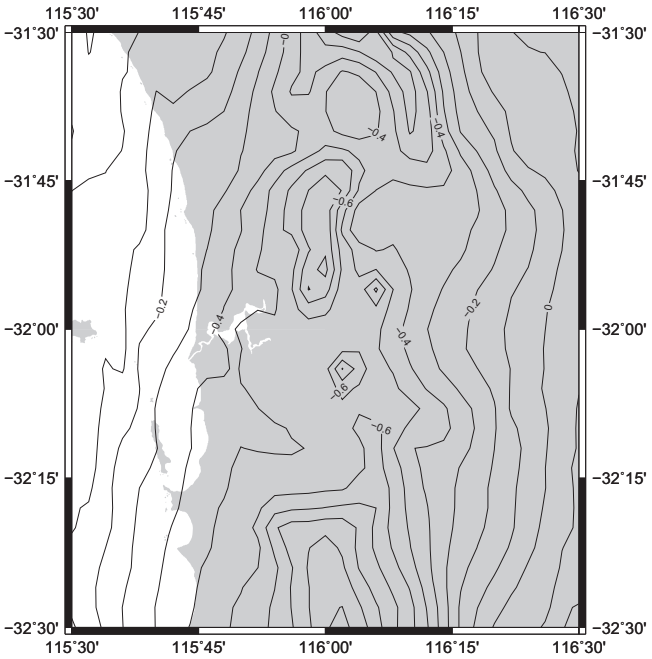

Fig. 11 Residual gravimetric quasigeoid from planar LSC with non-stationary covariances, relative to EGM2008 at the 99 GPS-levelling points [contour interval 0.1 m; Mercator projection]